Antibody-Mediated Targeting of a Hybrid Insulin Peptide Toward Neonatal Thymic Langerin-Positive Cells Enhances T-Cell Central Tolerance and Delays Autoimmune Diabetes

Yong Lin,[1] Jelena Perovanovic,[2] Yuelin Kong,[1] Botond Z. Igyarto,[3] Sandra Zurawski,[4] Dean Tantin,[2] Gerard Zurawski,[4] Maria Bettini,[2] and Matthew L. Bettini[2]

Diabetes 2022;71:1735–1745 | https://doi.org/10.2337/db21-1069

Thymic presentation of self-antigens is critical for establishing a functional yet self-tolerant T-cell population. Hybrid peptides formed through transpeptidation within pancreatic β-cell lysosomes have been proposed as a new class of autoantigens in type 1 diabetes (T1D). While the production of hybrid peptides in the thymus has not been explored, due to the nature of their generation, it is thought to be highly unlikely. Therefore, hybrid peptide-reactive thymocytes may preferentially escape thymic selection and contribute significantly to T1D progression. Using an antibody-peptide conjugation system, we targeted the hybrid insulin peptide (HIP) 2.5HIP toward thymic resident Langerin-positive dendritic cells to enhance thymic presentation during the early neonatal period. Our results indicated that anti–Langerin-2.5HIP delivery can enhance T-cell central tolerance toward cognate thymocytes in NOD.BDC2.5 mice. Strikingly, a single dose treatment with anti–Langerin-2.5HIP during the neonatal period delayed diabetes onset in NOD mice, indicating the potential of antibody-mediated delivery of autoimmune neoantigens during early stages of life as a therapeutic option in the prevention of autoimmune diseases.

Type 1 diabetes (T1D) is an autoimmune disease resulting from T cell–mediated destruction of pancreatic β-cells (1). Early studies on the variable number tandem repeat sequence in the insulin gene promoter suggested an association between β-cell antigen expression in the thymus and risk of developing T1D (2,3). This observation led to the hypothesis that decreased thymic presentation of β-cell antigens weakens T-cell central tolerance of the diabetogenic T-cell population, increasing risk for T1D. Hybrid peptides are a novel class of diabetogenic autoantigens (4,5). The search for self-antigens targeted by blood dendritic cell (BDC) diabetogenic T-cell clones in a NOD mouse model of T1D led to the identification of highly stimulatory hybrid peptides formed by peptide fusion within β-cell granules (6). These hybrid epitopes have since been identified in both mice and humans (6,7). Importantly, T cells reactive to hybrid peptides are indicative of disease activity in the NOD model (4,8). Owing to the nature of hybrid peptide generation, it is unlikely that the source peptide fragments from two different β-cell proteins are available in sufficient quantity in the thymus for the reaction to proceed. Therefore, it is hypothesized that hybrid peptide-reactive thymocytes are more likely to escape thymic selection and contribute significantly to T1D progression.

To elucidate the contribution of altered thymic tolerance to hybrid peptides in autoimmune diabetes, we devised a strategy to enhance the thymic presentation of the hybrid insulin peptide (HIP) 2.5HIP at an early neonatal stage of NOD mouse development, before significant thymic egress of αβ T cells. 2.5HIP (LQTLALWSRMD) is identified as the target antigen for the diabetogenic T-cell clone BDC2.5 (6).

[1]Baylor College of Medicine, Houston, TX
[2]Department of Pathology, University of Utah, Salt Lake City, UT
[3]Department of Microbiology and Immunology, Thomas Jefferson University, Philadelphia, PA
[4]Baylor Institute for Immunology Research, Baylor Scott and White Research Institute, Dallas, TX

Corresponding author: Matthew L. Bettini, matt.bettini@path.utah.edu

Received 23 November 2021 and accepted 16 May 2022

This article contains supplementary material online at https://doi.org/10.2337/figshare.19799728.

The epitope is formed through the fusion of peptide fragments from proinsulin and chromogranin-A (ChgA), two β-cell autoantigens critical for diabetes development in the NOD mouse (9,10). However, the contribution of their hybrid, 2.5HIP, to diabetes progression is unclear. Here, we conjugated 2.5HIP to an anti-Langerin antibody, which can then target the peptide to the Langerin-expressing thymic resident dendritic cells (DCs) for presentation to thymocytes. Ectopic expression of an autoimmune regulator (AIRE)-dependent β-cell antigen in thymic antigen-presenting cells (APCs) was shown to enhance T-cell central tolerance of the responsive thymocytes, resulting in protection from T1D (11). Additionally, a previous study targeting peptides to peripheral Langerin-positive DCs induced a robust increase in antigen-specific Foxp3$^+$ cells, suggesting potentially similar role for Langerin-positive DCs in thymic regulatory T cell (tTreg) development (12). We hypothesized that anti-Langerin antibody-mediated delivery of 2.5HIP to neonatal thymic Langerin-positive DCs can enhance T-cell central tolerance of 2.5HIP-reactive thymocytes, resulting in delayed diabetes onset. In the NOD.BDC2.5 model, our results indicate peptide delivery into the neonatal thymus can enhance negative selection and Foxp3$^+$ tTreg development. Similarly, in the wild-type polyclonal setting, we observed a consistent enhancement in the negative selection of cognate thymocytes associated with partial protection against diabetes development.

RESEARCH DESIGN AND METHODS

Mice

NOD/ShiLtJ (NOD), NOD.BDC2.5, B6.Rag2GFP, NOD.*scid*, and NOD.CD45.2 mice were purchased from The Jackson Laboratory and maintained at the Baylor College of Medicine and University of Utah animal facility under specific pathogen-free conditions. All experimental protocols were approved by The University of Utah's Institutional Animal Care and Use Committee.

Antibody-Peptide Conjugation and Intraperitoneal Injection

The anti-Langerin antibody (clone 4C7) containing the dockerin domain (Ab-dockerin) and cohesin-CG-thiopyridine were provided by the Zurawski laboratory (Baylor Institute for Immunology Research). The addition of the dockerin domain to an antibody and modifications to abrogate Fc receptor interactions were described previously (13). The 2.5HIP peptide, LQTLALWSRMD, with a C-terminal cysteine (2.5HIP-cysteine) was purchased from GenScript. To generate the complete anti–Langerin-dockerin:cohesin-2.5HIP conjugate (Ab-2.5HIP), the cohesin-2.5HIP conjugate was first made by incubating the 2.5HIP-cysteine peptide with cohesin-CG-thiopyridine overnight at room temperature. Ab-dockerin was then added to the cohesin-2.5HIP conjugate mixture and incubated for 30 min at room temperature in the presence of calcium-containing 1× Dulbecco's PBS (DPBS). After 30 min, the mixture was flowed through a 40-kD–MWCO Zeba Spin column (Thermo Fisher Scientific) to remove the unconjugated components. In all experiments, 2.5 μg of Ab-2.5HIP in 30 μL of 1× DPBS was injected intraperitoneally into 1- to 2-day-old neonates. The control (CTRL) groups were injected with DPBS, anti-Langerin antibody without the peptide (Ab-alone), or conjugated to OVA 323-339 peptide (Ab-OVA).

Diabetes Monitoring

Urine glucose level was evaluated by Diastix (Ascensia Diabetes Care). Hyperglycemia was confirmed by blood glucose level using a FreeStyle Lite glucometer (Abbott). Blood glucose level of >400 mg/dL or >300 mg/dL over 2 consecutive days was considered diabetic. Female mice were used for all NOD wild-type diabetes-monitoring experiments.

Analysis of Recent Thymic Immigrants

NOD.BDC2.5 and B6.Rag2GFP mice were crossed, and neonatal male and female F2 NOD/B6.BDC2.5.RagGFP hybrids homozygous for I-Ag7 were used for the experiment.

Flow Cytometry Analysis

Single-cell suspensions of tissue samples were prepared by mechanically dissociating the organs between microscope slides and being resuspended in staining buffer (PBS, 3% v/v FCS, 0.05% w/v sodium azide). Single-cell suspension of pancreatic islets was prepared by enzymatic digestion of the pancreas. Briefly, the pancreas was perfused with 3 mL of a 600 units/mL collagenase IV (Worthington Biochemical) solution via the pancreatic duct. The pancreas was then extracted and placed into 3 mL of a 600 units/mL collagenase IV solution and incubated for 30 min at 37°C. Individual islets were picked under a microscope and further dissociated using the enzyme-free cell dissociation buffer (Gibco). Ghost V510 (TONBO) and FcBlock (BioLegend) were used to exclude dead cells and block nonspecific staining, respectively. Flow cytometry data were acquired on a BD LSRFortessa (Becton Dickinson) flow cytometer and analyzed using the FlowJo 10 software (FlowJo LLC). The following antibodies were used in this study: CD4 (GK1.5), CD8α (53-6.7), T-cell receptor (TCR) vβ (H57-597), CD3ε (145-2C11), cleaved caspase 3 (D3E9), Foxp3 (FJK-16s), CD73 (TY/11.8), CD25 (PC61), CD11c (N418), Langerin (4C7), and MHCII molecule I-Ag7 (39-10-8). 2.5HIP/I-Ag7 tetramer was supplied by the National Institutes of Health Tetramer Core Facility.

Thymus Transplant Surgery

NOD.*scid* and NOD.CD45.2 were bred to generate the NOD.*scid*.CD45.2 female recipients for the experiment. Female NOD.BDC2.5 neonates were used as donors. Two-day-old NOD.BDC2.5 neonates were injected intraperitoneally with Ab-alone or Ab-2.5HIP. The thymus was extracted the next day and immediately transplanted under the

kidney capsule, as previously described (14). Briefly, the recipient mouse was anesthetized, and the incision site was disinfected with topical antiseptics. An incision was made on the left flank to expose the kidney. Once the kidney was exposed, an incision was made in the kidney capsule, and half of a lobe of the thymus was inserted below the capsule. The incision openings were closed with an absorbable suture and wound clips for the peritoneum and skin, respectively. The mice were given analgesics and antibiotics postsurgery to minimize pain and infection.

Insulitis Scoring by Hematoxylin and Eosin

Pancreas was harvested from mice and immediately placed in 4% paraformaldehyde (Santa Cruz Biotechnology) for 36–48 h at 4°C. The tissues were then transferred into 70% ethanol and sent to the histology core for processing, embedding, and sectioning into 6-μm sections. For insulitis scoring, three tissue sections, separated by 150 μm between each section, were taken from each pancreas. The paraffin was dissolved by xylene and the tissue hydrated through graded ethanol solutions. The sections were then stained with Harris Hematoxylin (Poly Scientific R&D) and counterstained with eosin (Poly Scientific R&D) before dehydrating, clearing, and mounting the slides with Permount (Fisher Scientific). Microscopy images were acquired with the Axio Scan.Z1 Slide Scanner (Zeiss). Each pancreas sample was assigned randomized identification numbers prior to scoring and unmasked for the final aggregate analysis between treatment groups. Scoring criteria: 0 = no infiltrates, 1 = peri-islet infiltrates, 2 = intraislet infiltrates to ≤50%, and 3 = intraislet infiltrates to ≥50%.

Single-Cell RNA Sequencing Analysis

Three-day-old NOD.BDC2.5 neonates were treated with Ab-alone or Ab-2.5HIP. CD4SP and $CD4^+CD8^-$ intermediate thymocytes were sorted 72 h later for single-cell RNA sequencing (scRNAseq) analysis. Sequences from the chromium platform were demultiplexed and aligned using Cell Ranger 3.1 software (10x Genomics) with default parameters to mouse genome mm10 from Ensembl GRCm38. Clustering, filtering, variable gene selection, and dimensionality reduction were performed using Seurat 4.0.2 (15), according to the following workflow:

1. Cells with <200 and >4,000 detected genes were excluded from further analysis.
2. Cells with <10% unique molecular identifiers mapping to mitochondrial genes were retained for downstream analysis.
3. The unique molecular identifier counts per 10,000 were log-normalized for each cell using the natural logarithm.
4. Variable genes (2,000 features) were selected using the function FindVariableFeatures.
5. Common anchors between the treatment and CTRL condition were identified using the FindIntegrationAnchors function that was further used to integrate these sets.
6. The expression level of genes in the integrated set was scaled along each gene, and linear dimensional reduction was performed. The number of principle component analyses was decided through the assessment of statistical plots (JackStrawPlot and ElbowPlot).
7. Cells were clustered using a shared nearest neighbor modularity optimization-based clustering algorithm and visualized using two-dimensional uniform manifold approximation and projection.

Differential gene expression analysis between the treatment and CTRL clusters was performed using FindMarkers. Genes with adjusted P values of <0.05 and avg_log2FC >0.2 and <-0.2 were marked red on scatter plots.

Pseudotime trajectory analysis of scRNAseq was performed using Monocle3 v0.2.1 to determine the developmental relationship between the cell clusters based on known thymocyte maturation markers identified in each cluster (16). Treatment and CTRL sets were filtered, integrated, and clustered using Seurat. Clusters containing the most immature (cluster 6) and the most mature thymocytes (cluster 1) were identified based on differentially expressed genes. Setting cluster 6 (Seurat; integrated set) as the root_group, the pseudotime algorithm generated the developmental pathway from the most immature cells to the most mature cells and overlayed the path onto the uniform manifold approximation and projection plot. Cells were plotted using plot_cells function using color_cells_by = pseudotime.

Statistics

GraphPad Prism 8 was used for all statistical analyses of experiments except the scRNAseq data set. Data are represented as mean ± SD. Unless otherwise specified in the figure legend, P values were calculated using the Mann-Whitney U test for comparisons between two groups or Kruskal-Wallis and Dunn test for comparisons of more than two groups. Diabetes incidence was compared using the Gehan-Breslow-Wilcoxon test. A P value of <0.05 is considered significant.

Data and Resource Availability

The data sets generated during and/or analyzed during the current study are available from the corresponding author upon reasonable request.

RESULTS

Demonstrating Feasibility and Duration of Approach

Langerin is expressed by ∼50% of the $MHCII^+CD11c^+$ thymic population in young NOD neonates but is not expressed on thymic epithelial cells (Fig. 1*A* and Supplementary

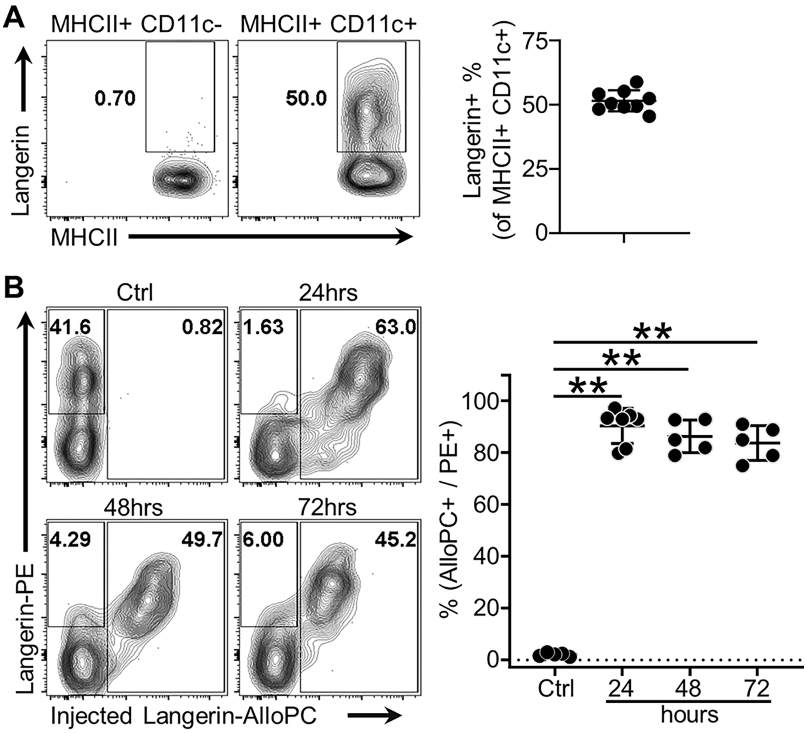

Figure 1—Anti–Langerin-fluorophore conjugate demonstrates feasibility and duration of approach. *A*: Representative flow plot and quantification of thymic Langerin-positive DC frequency in 2-day-old NOD neonates ($n = 9$). *B*: In vivo targeting of thymic Langerin-positive DCs by anti-Langerin antibody conjugated to the fluorophore APC. NOD neonates (2 days old) of both sexes were given 3 μg of anti-Langerin antibody conjugated to the fluorophore APC. Thymi were harvested at 24, 48, and 72 hours posttreatment. Data were pooled from three independent experiments; gated on $MHCII^+CD11c^+$; Ctrl = untreated; $n = 5$–7 per group). Data are mean ± SD. Mann-Whitney *U* test. $^{**}P < 0.01$.

Fig. 1). To examine the feasibility of antibody-mediated peptide targeting toward thymic Langerin-positive DCs, we injected 3 μg of anti-Langerin antibody conjugated to the fluorophore allophycocyanin (Langerin-AlloPC) intraperitoneally into 2-day-old NOD mice. Thymi were harvested at the indicated time points and costained with the anti-Langerin antibody conjugated to the fluorophore phycoerythrin (Langerin-PE). The percentage of Langerin-positive DCs targeted by the injected antibody (Langerin-$AlloPC^+$) was calculated as a percentage of the total Langerin-positive DCs (Langerin-PE^+). The results suggest that the antibody can target nearly all of the thymic Langerin-positive DCs within 24–72 h (Fig. 1*B*). To evaluate the duration of peptide presentation, we treated 1- to 2-day old NOD mice with 2.5 μg of Ab-2.5HIP, Ab-alone, or DPBS. At 1, 5, and 10 days posttreatment, we isolated thymic $CD11c^+$ DCs and cocultured with BDC2.5 T cells for 48 h. Assessing T-cell activation as an indication of peptide presentation, the data indicate minimal peptide presentation 5 days postinjection (Supplementary Fig. 2*A*). While peripheral Langerin-positive DCs were also targeted by the antibody (Supplementary Fig. 2*B*), the low number of peripheral T cells at the time of treatment (Supplementary Fig. 2*C*) and the rarity of antigen-specific T-cell clones suggest that it is unlikely that any observed tolerogenic effects result from enhanced peripheral tolerance, although it cannot be completely ruled out.

Targeting 2.5HIP to Thymic Langerin-positive DCs Enhances T-Cell Central Tolerance in the NOD.BDC2.5 Mouse

To evaluate thymocyte development, we treated 2-day-old NOD.BDC2.5 neonates with 2.5 μg of Ab-2.5HIP, Ab-alone, or DPBS and assessed thymocyte response 72 h later. Compared with CTRL, the Ab-2.5HIP group showed reduced thymic cellularity (Fig. 2*A*). A decrease in frequency and total number of $CD4^+CD8^+$ double-positive (DP) thymocytes as well as an increase in CD69 expression at this stage were observed (Fig. 2*B* and Supplementary Fig. 3*A*), suggesting enhanced negative selection at the DP stage. The increase in the percentage of CD4 single-positive (CD4SP) thymocytes is likely due to the decrease in the DP cells and not to an increase in the cellularity of the CD4SP population (Fig. 2*B*, top right). We also assessed T-cell central tolerance by quantifying Foxp3 (tTreg development) and cleaved caspase 3 (cCasp3; negative selection) expression in CD4SP thymocytes. We observed an antigen-specific increase of both the $Foxp3^+$ (Fig. 2*C* and Supplementary Fig. 4*A*) and $cCasp3^+$ cells (Fig. 2*D* and Supplementary Fig. 4*B*) within the CD4SP thymocytes after Ab-2.5HIP

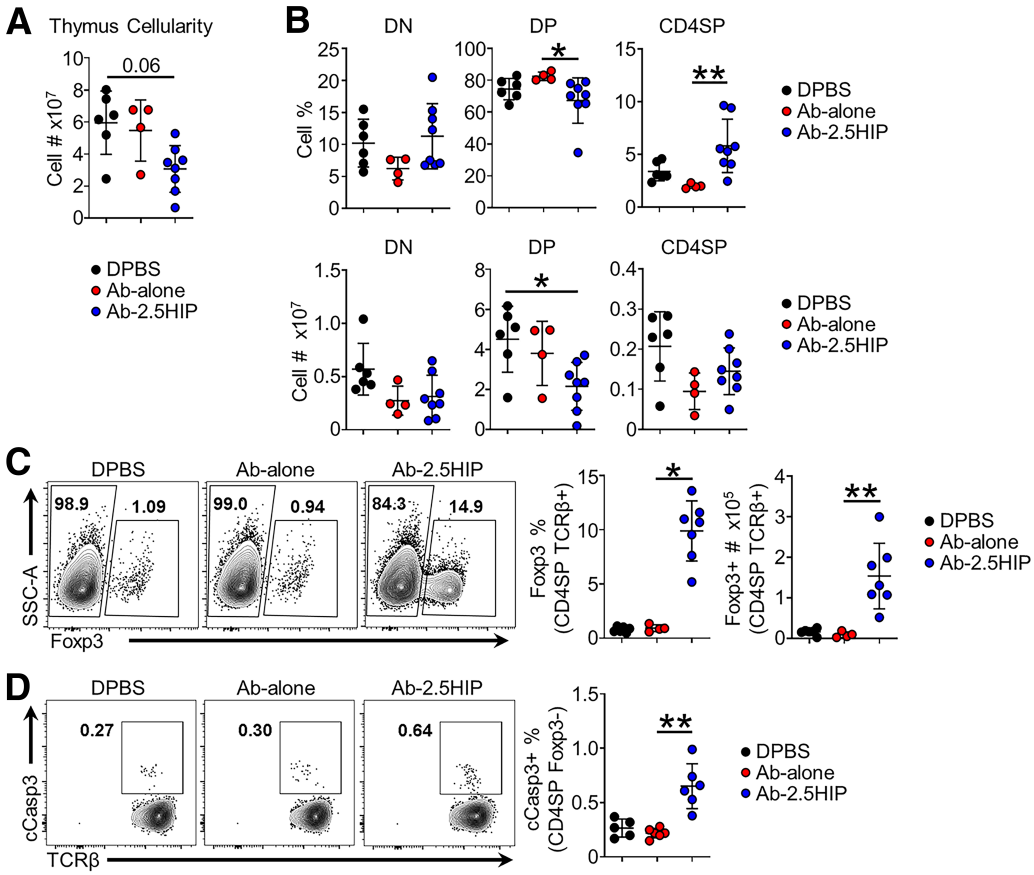

Figure 2—Anti–Langerin-2.5HIP alters thymocyte development, increasing thymocyte apoptosis and Foxp3$^+$ thymocyte population in BDC2.5 neonatal thymus. *A*: Total thymus cell count (n = 4–8 mice per group). *B*: Frequency and total number of thymocytes in the CD4$^-$CD8$^-$ (DN), CD4$^+$CD8$^+$ (DP), and CD4$^+$CD8$^-$ (CD4SP) stages of thymocyte development 72 h posttreatment. *C*: Representative flow plot and quantification of Foxp3$^+$ cell percentage and number within CD4SP TCRβ$^+$ thymocytes (n = 4–7 mice per group). SSC-A, side scatter area. *D*: Representative flow plot of apoptotic cell percentage within CD4SP TCRβ$^+$ Foxp3$^-$ thymocytes (n = 5–6 mice per group). Data were pooled from at least two independent experiments and are reported as mean ± SD. Kruskal-Wallis and Dunn tests. *$P < 0.05$, **$P < 0.01$.

treatment. Overall, these data suggest that delivery of antigen, in this targeted manner can enhance T-cell central tolerance of the responsive thymocytes.

Ab-2.5HIP–Induced Tregs Are Thymically Derived and Are of the CD25$^-$ Lineage

It has been reported that T cells from the periphery can recirculate back into the thymus (17). Therefore, we evaluated whether Ab-2.5HIP–induced Tregs were derived from thymocytes or from recirculating T cells by CD73 expression, where CD73$^-$ indicates thymocytes (18). The results indicate that ∼95% of the Ab-2.5HIP–induced tTregs are CD73$^-$ (Fig. 3*A*), indicating a thymocyte origin.

tTregs arise from two progenitor populations, one expressing the α-chain of the high-affinity interleukin 2 (IL-2) receptor (CD25) but not Foxp3, and the other expressing Foxp3 but not CD25 (18). Interestingly, Ab-2.5HIP induced tTregs that lacked CD25 expression, suggesting Foxp3$^+$CD25$^-$ developmental lineage (Fig. 3*B*). The accumulation of Foxp3$^+$CD25$^-$ thymocytes was perplexing, given that tTreg precursors depend on the common γ-chain–mediated cytokine signaling for survival (19). To determine whether the Ab-2.5HIP–induced tTregs are prone to apoptosis, we evaluated the frequency of cCasp3$^+$ cells within the Treg population. Although lacking CD25 expression, we did not detect an increased frequency of apoptotic cells within the Ab-2.5HIP group (Fig. 3*C*), suggesting Ab-2.5HIP–induced tTregs can survive and exit the thymus. It is possible that higher expression of the IL-2 receptor β-chain (CD122) may compensate and support the survival of tTregs in the absence of CD25. However, Ab-2.5HIP–induced CD25$^-$ tTregs did not express elevated levels of CD122 (Supplementary Fig. 5), suggesting an alternate survival mechanism.

Using scRNAseq, we examined the Ab-2.5HIP–induced tTregs within the CD4SP thymocytes for possible mechanisms of survival (Supplementary Fig. 6*A*). Assessment of Foxp3 expression indicated that the majority of Ab-2.5HIP–induced Foxp3$^+$ cells are localized in clusters 1 and 5 (Supplementary Fig. 6*B* and *C*). To understand the developmental relationship among the clusters, we performed a pseudotime analysis (Supplementary Fig. 6*D*).

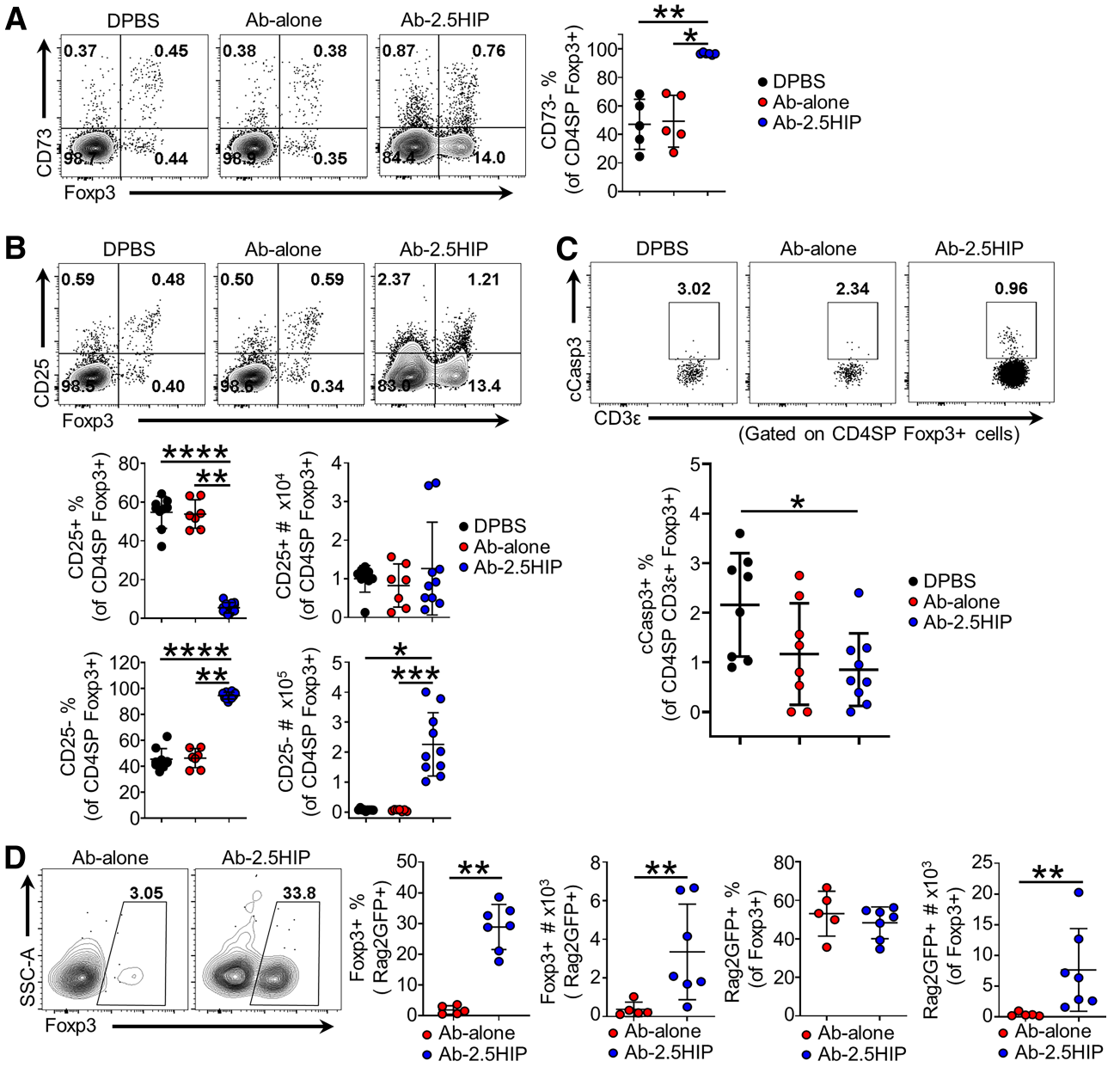

Figure 3—Ab-2.5HIP–induced BDC2.5 Tregs are thymically derived and are of the CD25− lineage. *A*: Representative flow plot and quantification of CD73 expression in Ab-2.5HIP–induced Foxp3$^+$ thymocytes 72 h posttreatment (n = 5–6 per group). *B*: Representative flow plot and quantification of Foxp3$^+$CD25$^+$ and Foxp3$^+$CD25$^-$ thymocytes (n = 7–10 per group). *C*: Representative flow plot and quantification of apoptotic cell frequency (gated on CD4SP Foxp3$^+$ cells; n = 8–9 per group). *D*: Representative flow plot and quantification of Foxp3$^+$ T cells within recent thymic emigrants (Rag2GFP$^+$ cells) 6 days after Ab-2.5HIP treatment in BDC2.5.Rag2GFP neonates (n = 5–7 per group). SSC-A, side scatter area. Data represent three independent experiments (*A–C*) and two independent experiments (*D*) and are reported as mean ± SD. Kruskal-Wallis and Dunn Tests (*A–C*), and Mann-Whitney *U* test (*D*). *P < 0.05, **P < 0.01, ***P < 0.001, ****P < 0.0001.

The most immature cells (expression of *Cd8b1* and *Rag2*) were identified in cluster 6. The most mature cells were localized in cluster 1 (expression of *Sell* and *S1pr*). The data suggest the generation of Ab-2.5HIP–induced tTregs in cluster 5, followed by maturation within cluster 1. Among the differentially expressed genes in cluster 5 of the treatment group is *Tnfrsf4* (OX40) (Supplementary Fig. 6*E*), which has been reported to promote the survival and expansion of Tregs (20,21). Costimulation by OX40L in tTreg progenitors was shown to enhance their sensitivity to IL-2 signaling (22). Therefore, Ab-2.5HIP–induced tTregs may be more sensitive to IL-2 despite low levels of CD25 expression.

To verify Ab-2.5HIP–induced tTregs survive and egress from the thymus, we assessed Treg frequency within BDC2.5 recent thymic emigrants (RTEs) in the spleen 6 days after Ab-2.5HIP treatment, as they are the least likely to be influenced by the peripheral environment at

this early time point. To assess RTEs, we crossed the B6.Rag2EGFP transgenic mouse with the NOD.BDC2.5 strain. Gating on green fluorescent protein (GFP)-positive RTEs, we detected an increase in Foxp3$^+$ cells in response to Ab-2.5HIP treatment (Fig. 3*D*), further indicating that Ab-2.5HIP–induced tTregs can survive and exit the thymus. While Ab-2.5HIP–induced tTregs in the thymus were CD25$^-$, we observed an increase in both the Foxp3$^+$CD25$^+$ and Foxp3$^+$CD25$^-$ Tregs within the RTE population (Supplementary Fig. 7*A*). It is possible that Ab-2.5HIP–induced tTregs upregulate CD25 upon thymic egress or that CD25$^+$ Tregs selectively expand in the periphery. Similar to the RTEs, an increase in Foxp3$^+$ cells was also detected in the non-RTEs within the spleen (Supplementary Fig. 7*C*), suggesting potential induction of Tregs by peripheral Langerin-positive DCs, although we cannot exclude the loss of GFP through proliferation and GFP degradation.

Ab-2.5HIP–Enhanced Central Tolerance Delays Diabetes in an Accelerated Diabetes Model

To address whether Ab-2.5HIP–induced thymic changes have any effect on diabetes incidence, we adapted an accelerated diabetes induction model, mediated by BDC2.5 T-cell transfer into NOD.*scid* recipients (23). In our modified protocol, we transplanted NOD.BDC2.5 thymi from 3-day-old neonates that were treated with Ab-2.5HIP or Ab-alone (Fig. 4*A*). We observed a delay in diabetes onset of ~5–6 weeks within the Ab-2.5HIP group, indicating delayed destruction of β-cells (Fig. 4*B*). This delay was consistent with the observed higher islet counts and reduced insulitis severity in the Ab-2.5HIP group 2 weeks posttransplant (Fig. 4*C*). To account for the delayed destruction of β-cells, we assessed changes in donor T-cell phenotype in the periphery posttransplant. At 2 weeks posttransplant, we observed a decrease in the donor T-cell frequency in the spleens and the axillary lymph nodes (aLNs) in the Ab-2.5HIP group (Fig. 4*D*), indicating delayed accumulation of donor T cells due to enhanced thymic deletion and/or delayed thymic emigration. However, Ab-2.5HIP did not upregulate CD69 in CD4SP thymocytes (Supplementary Fig. 3*B*), suggesting Ab-2.5HIP did not impede thymocyte migration via the S1PR1-CD69 interaction (24,25). In contrast, no difference in donor T-cell frequency was observed in the pancreatic lymph node (pLN), likely due to the presence of antigen in all groups driving T-cell accumulation.

Analysis of donor Tregs showed higher Treg frequencies across all organs within the Ab-2.5HIP group (Fig. 4*E*). However, an increase in Treg numbers was observed only in the pLN (Supplementary Fig. 8*A*, bottom). While the Treg numbers do appear to increase at 6 weeks posttransplant (Supplementary Fig. 8*B*), the Treg frequency is mostly unchanged except for a nonsignificant decrease in the spleen (Supplementary Fig. 8*C*). Therefore, the eventual onset of diabetes in this model is not due to a lack of persistence of Ab-2.5HIP Tregs but is perhaps due to the increased activation of BDC2.5 Teff (CD62L$^-$ CD44$^+$) by 6 weeks posttransplant (Supplementary Fig. 8*D*). Low CD25 expression on Tregs was not correlated with eventual disease development, as CD25 was upregulated by 6 weeks (Supplementary Fig. 8*E*). While the relative contribution of Ab-2.5HIP–enhanced thymic deletion and tTreg generation cannot be distinguished in this transplant model, both processes likely contributed to the delayed disease onset through reduced donor T-cell accumulation and activation in the periphery.

Ab-2.5HIP Treatment in NOD Wild-Type Neonates Decreases 2.5HIP-Reactive Thymocyte Number and Delays Diabetes Onset

To assess the impact of Ab-2.5HIP treatment on the development of polyclonal T cells, we treated 1-day-old NOD wild-type mice with Ab-2.5HIP. Thymocyte response was assessed 3 days later by 2.5HIP tetramers. Compared with the CTRL group, we observed a significant decrease in the number of 2.5HIP-specific CD4SP thymocytes in the Ab-2.5HIP group (Fig. 5*A*), indicating enhanced negative selection. In contrast to thymocyte response in the NOD.BDC2.5 mouse, we did not detect a consistent increase in the Foxp3$^+$ frequency within the tetramer-positive population, possibly due to the overall low tetramer-positive cell number (Fig. 5*B*).

We next evaluated the long-term cumulative tolerogenic effect of Ab-2.5HIP treatment in neonates and its impact on diabetes development. To observe diabetes incidence, we injected Ab-2.5HIP into 1-day-old NOD wild-type females and monitored diabetes for 30 weeks. The single Ab-2.5HIP injection imparted an overall 20% reduction in diabetes incidence, which was associated with a delay in diabetes onset of ~5 weeks (Fig. 5*C*). To address the mechanism of protection, we examined 2.5HIP tetramer-positive cells in the periphery of NOD wild-type mice 10 weeks after treatment with Ab-2.5HIP. There was not a significant difference in the frequency of tetramer-positive cells among the groups in the pLN, but there was a slight decrease in the total number of tetramer-positive cells after treatment (Fig. 5*D*). Importantly, we detected a significant increase in the frequency of Foxp3$^+$ cells within the tetramer-positive population in the pLNs of Ab-2.5HIP–treated mice, suggesting a change in cellular composition of tetramer-positive population rather than reduction of cell numbers (Fig. 5*E*). Within the pancreatic islets, we observed a significant decrease in the frequency of CD4$^+$CD3$^+$ T cells in the Ab-2.5HIP group (Fig. 5*F*, left), which is associated with a decrease in total number of 2.5HIP tetramer-positive cells in the islets (Fig. 5*F*, right). However, only a few mice showed an increase in 2.5HIP tetramer-positive Foxp3$^+$ cell frequency in the islets (Fig. 5*G*, left). These results suggest enhanced immunosuppression due to increased 2.5HIP tetramer-positive Foxp3$^+$ cell frequency within the pLN led to a decrease in CD4 T-cell infiltration into the pancreatic islets.

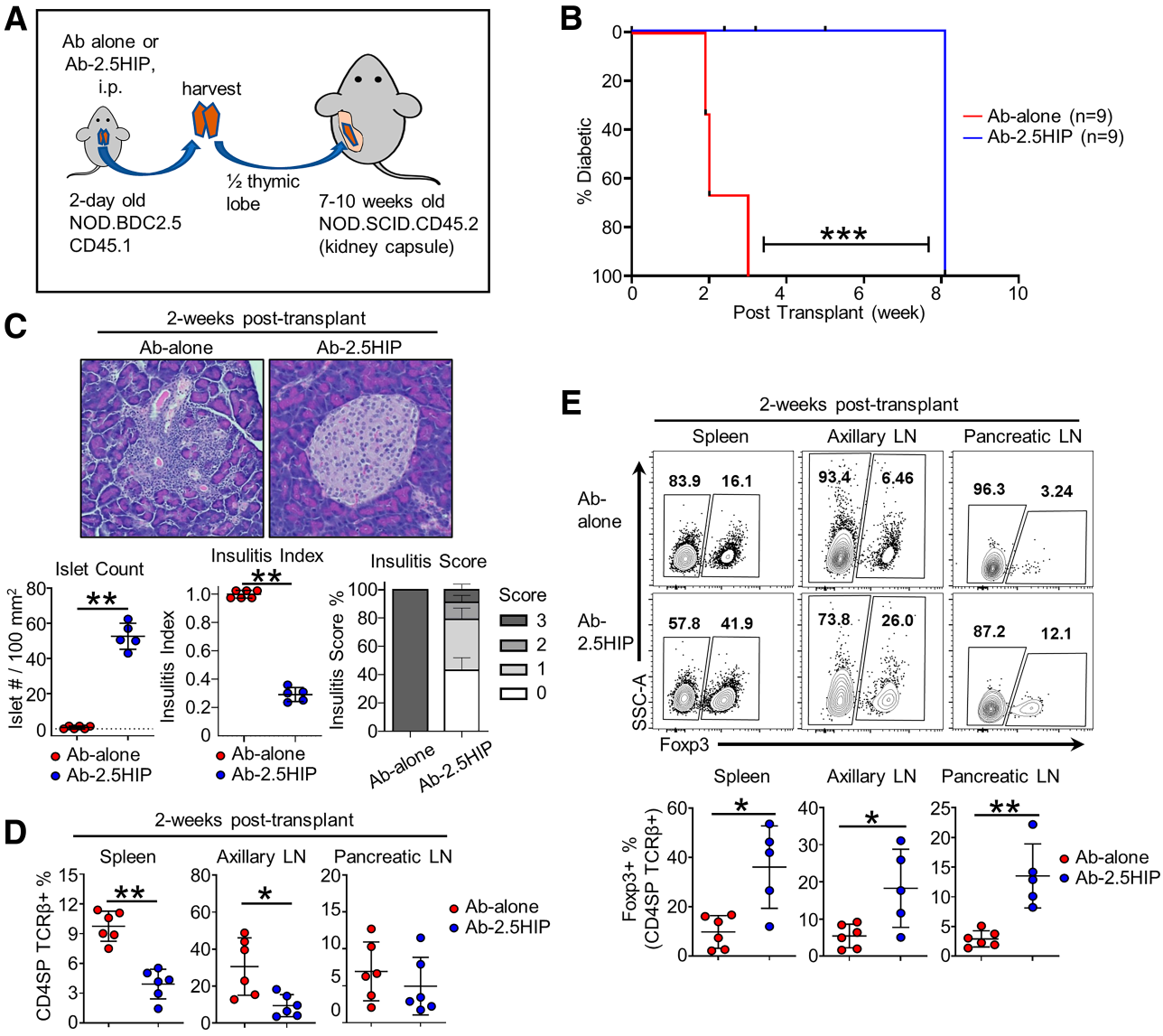

Figure 4—Ab-2.5HIP treatment leads to reduced diabetes incidence in a BDC2.5 thymus transplant model. *A*: Thymus transplant experimental design. *B*: Diabetes incidence of the thymus transplant recipients ($n = 9$ per group). *C*: Insulitis evaluation of thymus transplant recipients at 2 weeks posttransplant (insulitis score: 0 = no infiltrates, 1 = peri-islet infiltrates, 2 = intraislet infiltrates to ≤50%, 3 = intraislet infiltrates to ≥50%; $n = 5$–6 per group; data from two independent experiments). *D*: Quantification of donor CD4 T-cell percentage in the spleen, aLN, and pLN 2 weeks after thymus transplant ($n = 6$ per group). *E*: Representative flow plot and quantification of Foxp3$^+$ cell percentage in the spleen, aLN, and pLN 2 weeks after thymus transplant ($n = 5$–6 per group). Data are reported as mean ± SD. Mann-Whitney *U* test (*C*–*E*) and Gehan-Breslow-Wilcoxon test (*E*). *$P < 0.05$, **$P < 0.01$, ***$P < 0.001$.

DISCUSSION

We sought to determine whether enhanced thymic presentation of a single neoantigen can alter autoimmunity later in life. We enhanced thymic presentation of 2.5HIP in NOD neonates through an anti-Langerin Ab-mediated targeting of 2.5HIP to thymic Langerin-positive DCs. After a single dose of Ab-2.5HIP, we observed a reduction of 2.5HIP-reactive thymocytes, which correlated with an increase in 2.5HIP-reactive Treg frequency in the periphery at 10 weeks of age and a 5-week delay in the age of diabetes onset (Fig. 5). Considering the difference in disease protection between our results and in the ChgA-knockout mouse, 2.5HIP reactivity may not fully explain the nearly complete protection from diabetes seen in the ChgA-knockout mouse. Indeed, while 2.5HIP is the only ChgA-derived HIP identified in vivo thus far, other ChgA-derived hybrid peptides were also shown to stimulate diabetogenic T-cell clones in vitro (26). Further, prior work revealed a role for ChgA in granule formation within endocrine cells (27,28). In β-cells, ChgA were shown to affect insulin secretion (29,30). A reduction in insulin-derived peptide presentation was also reported in the ChgA-knockout mouse, potentially

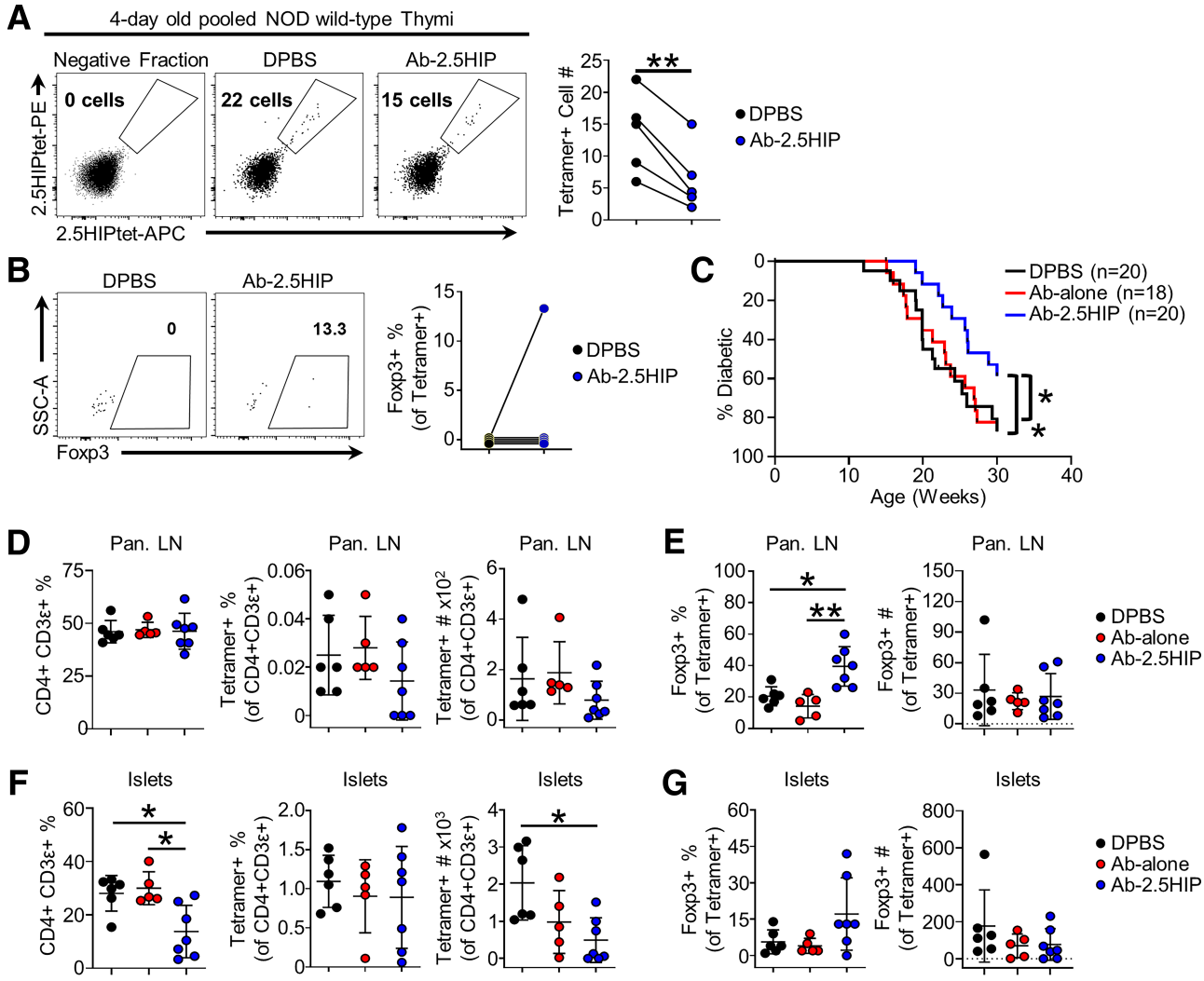

Figure 5—Ab-2.5HIP treatment in NOD wild-type neonates enhances T-cell central tolerance and delays diabetes onset. *A*: 2.5HIP tetramer analysis of CD4SP thymocytes 72 h after treatment of 1-day-old NOD wild-type neonates with Ab-alone or Ab-2.5HIP ($n = 5$ per group). Each data point represents three to five pooled thymi enriched for 2.5HIP-reactive cells by tetramer; data represent 5 independent experiments. *B*: Frequency of Foxp3$^+$ cells within tetramer-positive cells. SSC-A, side scatter area. *C*: Diabetes incidence of NOD wild-type female mice treated with a single 2.5-μg dose of Ab-alone or Ab-2.5HIP at 1 day old ($n = 18$–20 per group). *D*: Quantification of CD4 T cells and 2.5HIP tetramer-positive T cells in the pLN at 10 weeks after treatment. *E*: Quantification of Foxp3$^+$ cells within 2.5HIP tetramer-positive T cells in the pLN at 10 weeks after treatment. *F*: Quantification of CD4 T cells and 2.5HIP tetramer-positive T cells in the pancreatic islets 10 weeks after treatment. *G*: Quantification of Foxp3$^+$ cells within 2.5HIP tetramer-positive T cells in the pancreatic islets at 10 weeks after treatment. (*D*–*G*: $n = 5$–7 per group; data from two independent experiments). Data are reported as mean ± SD. Paired *t* test (*A* and *B*), Gehan-Breslow-Wilcoxon Test (*C*), and Kruskal-Wallis and Dunn test (*D*–*G*). $^*P < 0.05$, $^{**}P < 0.01$.

affecting T-cell response against other β-cell autoantigens (31). Therefore, it is not unexpected to observe a difference in disease protection between our study and what was seen in the ChgA-knockout mouse. On the other hand, it is possible that we did not capture the full contribution of 2.5HIP reactivity to diabetes progression given the short treatment duration. Nevertheless, significant protection due to a single injection in neonates adds support to the idea of a critical neonatal window for establishing tolerance (32). Longer treatment duration may enhance the tolerogenic effect. However, how T cells response to 2.5HIP targeted to peripheral Langerin-positive DCs will need to be assessed. Mutating the 2.5HIP peptide to prevent its presentation may be necessary to determine the full contribution of 2.5HIP reactivity to disease progression.

In this study we targeted 2.5HIP toward Langerin-positive thymic DCs. Targeting peptides to other thymic APCs, such as the migratory DCs (Sirpα$^+$ and plasmacytoid DC antigen-1–positive [PDCA-1$^+$] DCs), may lead to different thymocyte fates. The thymocyte response is likely to be influenced by a variety of factors: differential expression of endocytic receptors between thymic DC subsets, relative proportion of thymic DC subsets, localization of the DC subsets within the thymus, and the DC subsets' propensity to promote negative selection versus tTreg development. Differential expression of endocytic

receptors will influence the choice of antibody targets and may affect the efficiency of antigen presentation (33). Thymic DC subset frequencies change with age (34), which may affect the amount and duration of peptide presentation. Unlike the resident and PDCA-1$^+$ DC subsets, the Sirpα$^+$ subset can also be found in the thymic cortex (35). Targeting peptides to the Sirpα$^+$ subset may preferentially result in the deletion of antigen-specific thymocytes at the DP stage. In vivo studies suggest that both the Sirpα$^+$ and PDCA-1$^+$ subsets were capable of inducing negative selection, but only the Sirpα$^+$ subset of DCs has been reported to participate in tTreg generation (36,37). These and other factors may be helpful in guiding the design of antibody-mediated peptide-targeting approaches to achieve a desired thymocyte response for therapeutic aims.

Acknowledgments. The authors would like to thank technicians in their laboratory for animal husbandry and maintenance. They would also like to acknowledge the University of Utah Cell Imaging Core for use of the Axio Scan.Z1 Slide Scanner microscope and thank Dr. Xiang Wang, Dr. Michael J. Bridge, and Joel M. Sederstrom for their assistance.

Funding. This study was supported by the National Institutes of Health (NIH) National Institute of Diabetes and Digestive and Kidney Diseases (grant 1R01DK114456), JDRF (grant 1-17-JDF-013), The Robert and Janice McNair Foundation, NIH National Institute of Allergy and Infectious Diseases (1R01AI125301 and R01AI100873), and NIH National Institute of General Medical Sciences (R01GM122778). Cell sorting for scRNAseq was supported by the Baylor College of Medicine Cytometry and Cell Sorting Core with funding from the Cancer Prevention & Research Institute of Texas (CPRIT) Core Facility Support Award (CPRIT-RP180672), the NIH National Cancer Institute (CA125123), and National Center for Research Resources (RR024574).

Duality of Interest. No potential conflicts of interest relevant to this article were reported.

Author Contributions. Y.L. executed the experiments. Y.L. and J.P. drafted the initial manuscript. Y.L., D.T., M.B., and M.L.B. edited the manuscript. Y.L. and M.L.B. conceptualized and designed the experiments. J.P. and D.T. guided and analyzed the scRNAseq data set. Y.K. assisted with diabetes incidence monitoring. B.Z.I., S.Z., and G.Z. generated the antibody-dockerin conjugate and cohesin reagents. M.B. provided guidance for data analysis and research directions. M.L.B. is the guarantor of this work and, as such, had full access to all the data in the study and takes responsibility for the integrity of the data and the accuracy of the data analysis.

Prior Presentation. Parts of this study were presented in abstract form at the 78th Scientific Sessions of the American Diabetes Association, Orlando, FL, 22–26 June 2018; and in abstract and poster form at the Immunology 2018 Meeting of the American Association of Immunologists, Austin, TX, 4–8 May 2018; and at the Immunology 2021 Meeting of the American Association of Immunologists, virtual conference, 10–15 May 2021.

References

1. Katsarou A, Gudbjörnsdottir S, Rawshani A, et al. Type 1 diabetes mellitus. Nat Rev Dis Primers 2017;3:17016

2. Pugliese A, Zeller M, Jr AF, et al. The insulin gene is transcribed in the human thymus and transcription levels correlated with allelic variation at the NS VNTR-IDDM2 susceptibility locus for type 1 diabetes. Nat Genet 1997;15:293–297

3. Vafiadis P, Bennett ST, Todd JA, et al. Insulin expression in human thymus is modulated by INS VNTR alleles at the IDDM2 locus. Nat Genet 1997;15:289–292

4. Mitchell AM, Alkanani AA, McDaniel KA, et al. T-cell responses to hybrid insulin peptides prior to type 1 diabetes development. Proc Natl Acad Sci U S A 2021;118:e2019129118

5. Wiles TA, Delong T. HIPs and HIP-reactive T cells. Clin Exp Immunol 2019;198:306–313

6. Delong T, Wiles TA, Baker RL, et al. Pathogenic CD4 T cells in type 1 diabetes recognize epitopes formed by peptide fusion. Science 2016;351:711–714

7. Wiles TA, Powell R, Michel R, et al. Identification of hybrid insulin peptides (HIPs) in Mouse and Human Islets by Mass Spectrometry. J Proteome Res 2019;18:814–825

8. Baker RL, Jamison BL, Wiles TA, et al. CD4 T cells reactive to hybrid insulin peptides are indicators of disease activity in the NOD mouse. Diabetes 2018;67:1836–1846

9. Baker RL, Bradley B, Wiles TA, et al. Cutting edge: nonobese diabetic mice deficient in chromogranin a are protected from autoimmune diabetes. J Immunol 2016;196:39–43

10. Nakayama M, Abiru N, Moriyama H, et al. Prime role for an insulin epitope in the development of type 1 diabetes in NOD mice. Nature 2005;435:220–223

11. Lee T, Sprouse ML, Banerjee P, Bettini M, Bettini ML. Ectopic expression of self-antigen drives regulatory T cell development and not deletion of autoimmune T cells. J Immunol 2017;199:2270–2278

12. Idoyaga J, Fiorese C, Zbytnuik L, et al. Specialized role of migratory dendritic cells in peripheral tolerance induction. J Clin Invest 2013;123:844–854

13. Flamar A-L, Zurawski S, Scholz F, et al. Noncovalent assembly of anti-dendritic cell antibodies and antigens for evoking immune responses in vitro and in vivo. J Immunol 2012;189:2645–2655

14. Morillon YM 2nd, Manzoor F, Wang B, Tisch R. Isolation and transplantation of different aged murine thymic grafts. J Vis Exp 2015:e52709

15. Stuart T, Butler A, Hoffman P, et al. Comprehensive integration of single-cell data. Cell 2019;177:1888–1902.e21

16. Trapnell C, Cacchiarelli D, Grimsby J, et al. The dynamics and regulators of cell fate decisions are revealed by pseudotemporal ordering of single cells. Nat Biotechnol 2014;32:381–386

17. Kirberg J, Bosco N, Deloulme J-C, Ceredig R, Agenès F. Peripheral T lymphocytes recirculating back into the thymus can mediate thymocyte positive selection. J Immunol 2008;181:1207–1214

18. Owen DL, Mahmud SA, Sjaastad LE, et al. Thymic regulatory T cells arise via two distinct developmental programs. Nat Immunol 2019;20:195–205

19. Tai X, Erman B, Alag A, et al. Foxp3 transcription factor is proapoptotic and lethal to developing regulatory T cells unless counterbalanced by cytokine survival signals. Immunity 2013;38:1116–1128

20. Bourdon J-C, Renzing J, Robertson PL, Fernandes KN, Lane DP. Scotin, a novel p53-inducible proapoptotic protein located in the ER and the nuclear membrane. J Cell Biol 2002;158:235–246

21. Kumar P, Marinelarena A, Raghunathan D, et al. Critical role of OX40 signaling in the TCR-independent phase of human and murine thymic Treg generation. Cell Mol Immunol 2019;16:138–153

22. Mahmud SA, Manlove LS, Schmitz HM, et al. Costimulation via the tumor-necrosis factor receptor superfamily couples TCR signal strength to the thymic differentiation of regulatory T cells. Nat Immunol 2014;15:473–481

23. Berry G, Waldner H. Accelerated type 1 diabetes induction in mice by adoptive transfer of diabetogenic CD4+ T cells. J Vis Exp 2013:e50389.

24. Feng C, Woodside KJ, Vance BA, et al. A potential role for CD69 in thymocyte emigration. Int Immunol 2002;14:535–544

25. Nakayama T, Kasprowicz DJ, Yamashita M, et al. The generation of mature, single-positive thymocytes in vivo is dysregulated by CD69 blockade or overexpression. J Immunol 2002;168:87–94

26. Reed B, Crawford F, Hill RC, et al. Lysosomal cathepsin creates chimeric epitopes for diabetogenic CD4 T cells via transpeptidation. J Exp Med 2021;218:e20192135

27. Mosley CA, Taupenot L, Biswas N, et al. Biogenesis of the secretory granule: chromogranin A coiled-coil structure results in unusual physical properties and suggests a mechanism for granule core condensation. Biochemistry 2007;46: 10999–11012
28. Koshimizu H, Cawley NX, Kim T, Yergey AL, Loh YP. Serpinin: a novel chromogranin A-derived, secreted peptide up-regulates protease nexin-1 expression and granule biogenesis in endocrine cells. Mol Endocrinol 2011;25:732–744
29. Tatemoto K, Efendić S, Mutt V, Makk G, Feistner GJ, Barchas JD. Pancreastatin, a novel pancreatic peptide that inhibits insulin secretion. Nature 1986;324:476–478
30. Schmid GM, Meda P, Caille D, et al. Inhibition of insulin secretion by betagranin, an N-terminal chromogranin A fragment. J Biol Chem 2007;282:12717–12724
31. Srivastava N, Hu H, Vomund AN, et al. Chromogranin A deficiency confers protection from autoimmune diabetes via multiple mechanisms. Diabetes 2021;70:2860–2870
32. Renz H, Adkins BD, Bartfeld S, et al. The neonatal window of opportunity-early priming for life. J Allergy Clin Immunol 2018;141:1212–1214
33. Hoober JK, Eggink LL, Cote R. Stories from the dendritic cell guardhouse. Front Immunol 2019;10:2880
34. Kroger CJ, Wang B, Tisch R. Temporal increase in thymocyte negative selection parallels enhanced thymic SIRPα^+ DC function. Eur J Immunol 2016;46: 2352–2362
35. Baba T, Nakamoto Y, Mukaida N. Crucial contribution of thymic Sirp $\alpha+$ conventional dendritic cells to central tolerance against blood-borne antigens in a CCR2-dependent manner. J Immunol 2009;183:3053–3063
36. Proietto AI, van Dommelen S, Zhou P, et al. Dendritic cells in the thymus contribute to T-regulatory cell induction. Proc Natl Acad Sci U S A 2008;105: 19869–19874
37. Hadeiba H, Lahl K, Edalati A, et al. Plasmacytoid dendritic cells transport peripheral antigens to the thymus to promote central tolerance. Immunity 2012;36:438–450